Supporting Information

Ru-anchoring Co-MOF-derived porous Ru-Co_3O_4 nanomaterials for enhanced oxygen evolution activity and structural stability

Nan Li,[a] Lujiao Mao,[a] Yuting Fu,[a] Haoran Wang,[a] Yuchang Shen,[a] Xuemei Zhou,[a,*] Qipeng Li,[b,*] and Jinjie Qian[a,*]

[a]Key Laboratory of Carbon Materials of Zhejiang Province, College of Chemistry and Materials Engineering, Wenzhou University, Wenzhou 325035, Zhejiang, P. R. China

[b]College of Chemistry and Chemical Engineering, Zhaotong University, Zhaotong 657000, Yunnan, P. R. China

*Corresponding author

E-mail: zxm.mei@163.com (X. Zhou), qpli@ztu.edu.cn (Q. Li); jinjieqian@wzu.edu.cn (J. Qian)

1. Experimental Details

1.1 Reagents and Materials.

Unless otherwise specified, chemicals are reagent grade and used without processing. Cobalt(II) acetate tetrahydrate ($Co(CH_3COO)_2 \cdot 4H_2O$, 99.5%, Aladdin), biphenyl-3,3',5,5'-tetracarboxylic acid (H_4BPTC, 98.0%, Jinan Henghua Technology Company), polyvinylpyrrolidone (PVP, ~58000, Aladdin), Ruthenium(III) chloride anhydrous ($RuCl_3$, Aladdin), N-Methylformamide (NMF, 99%, Aladdin), de-ionized water (18 MΩ), Nitric acid concentrated solution (HNO_3, 70%, Aladdin), and ethanol (EtOH, 95%, Aladdin).

1.2 Synthesis of CoOF-1 ($[Co_2(OH)_2(BPTC)]$)

The mixture of $Co(CH_3COO)_2 \cdot 4H_2O$ (30 mg, 0.12 mmol), H_4BPTC (0.05 mmol, 15 mg), NMF (2 mL), and EtOH (1 mL) are added to a 35 mL pressure-resistant tube. Meanwhile, HNO_3 (0.3 mL) solution can adjust the mixture to be acidic. The reaction is then in an aluminum block bath to 140 ^oC for 4h. After cooling to room temperature, the product was collected and centrifuged, washed three times with EtOH, and then the filtered solid was dried under vacuum at 85 ℃ overnight to obtain pure CoOF-1 in high yield.

1.3 Synthesis of Ru-CoOF-1

The mixture of CoOF-1 (30mg) and EtOH (3 mL) are added to a reaction kettle. Afterwards, certain volume of $RuCl_3$ solution (Ru wt.% =5 mg mL^{-1}) was transferred into the former mixture.Then placing them in a oven and heat at 140 ℃ for 6 h at a temperature increase rate of 1 ℃/min. After naturally cooling down to room

temperature, the products are collected and centrifuged, washed three times with EtOH, and then the filtered solid was dried under vacuum at 85 ℃ overnight to obtain Ru-CoOF-1.

1.4 Syntheses of Ru-Co_3O_4

The as-prepared Ru-CoOF-1 were weighted and placed in the muffle furnace. Then the temperature was set to 350 ℃ at a heating rate of 5 ℃ min^{-1} in air atmosphere and maintained for 6 h. The black powder was obtained after cooling to room temperature.According to the mass ratio of $RuCl_3$ to CoOF-1 (1:100, 5:100, and 10:100) in the preparation, the finally obtained Ru-incorporated Co_3O_4 catalysts were designated as Ru-Co_3O_4-x (x = 1, 5, and 10), respectively. The sample mainly involved in the characterization in this paper is Ru-Co_3O_4-5, which is referred to as Ru-Co_3O_4 for short.

2. Material Characterization

The microscopic and nanostructured morphologies of all samples are characterized by scanning electron microscopy (SEM, JEOL JSM-6700F, 10 kV). The powder X-ray diffraction (PXRD) patterns are collected on a Bruker D8 Advance at 40 kV and 40 mA with Cu Kα radiation (λ=0.154 nm). Thermogravimetric analysis (TGA) is implemented under a flowing N_2 atmosphere by using a NETZSCH STA 449C unit. Raman spectrometer is investigated on LabRAM HR Evolution from the 532 nm line of an Ar-ion laser. X-ray photoelectron spectroscopy (XPS) is recorded on a Thermo Scientific ESCALAB 250. Fourier transform infrared spectroscopy (FT-IR) spectra are carried on in the model of PerkinElmer Frontier MIR. N_2 adsorption/desorption

isotherms are used to characterize the determine specific surface areas and pore distribution of samples based on the Brunauer-Emmett-Teller method (BET, Micrometrics ASAP 2020 system).

3. Electrochemical measurements

All electrochemical data were collected via the CHI760E and/or Autolab electrochemical workstation. OER measurements were performed in 1.0 M KOH solution using a typical three-electrode system, the GCE (glassy carbon electrons) with catalyst ink, platinum mesh, and Hg/Hg_2Cl_2 electrode as the working electrode, counter electrode, and reference electrode, respectively. At the same time, we chose Hg/Hg_2Cl_2 as the reference electrode to ensure accuracy and reproducibility in alkaline media. All electrochemical tests in our work were performed without iR correction.

Briefly, the homogeneous catalyst ink was prepared by dispersing 2.5mg of catalyst powder into a mixed solution containing 75 μL of DI H_2O, 150 μL of ethanol and 25 μL of Nafion (5 wt.%), and then underwent an ultrasonic treatment for 1 h. 6 μL of the resultant catalyst ink was drop-casted onto the GCE electrode surface with a loading value of 0.85 mg cm^{-2},, and dried at room temperature. As a comparison, commercial RuO_2 also was tested.The linear sweep voltammetry (LSV) is collected with a scan rate of 5 mV s^{-1} after initial 40 circles cyclic voltammogram (CV) progress at a scan rate of 100 mV s^{-1} to have a stable CV curve.The electrochemical double-layer capacitance (C_{dl}) is measured by using CV in a non-faradaic region (0.91-1.01 V vs. RHE) at different scan rates of 20, 40, 60, 80 and 120 mV s^{-1}.

Electrocatalytic stability is made by using amperometric curve (i-t) at a potential of 1.5 V vs. RHE for 48 h.

4. Computational details

The construction models of CoOF-1 and Ru-CoOF-1 composites are optimized by the CASTEP module of Accelrys Materials Studio 2020 software to obtain the geometry optimizations structure with minimized energy, and the function is selected as Perdew-Burke Ernzerhof (PBE) in Generalized Gradient Approximation (GGA). The Brillouin zone is sampled with 2×2×2 k-points and cut-off energy of 489.80 eV is used. The formation energies (E_f) of Ru with different composites is calculated by the equation:

$$E_f = E_{Ru+sub} - E_{Ru} - E_{sub} \quad (1)$$

where E_{Ru+sub}, E_{Ru}, and E_{sub} are the energy of the CoOF-1 substance combined with the ruthenium, ruthenium atom, and CoOF-1 substance, respectively.

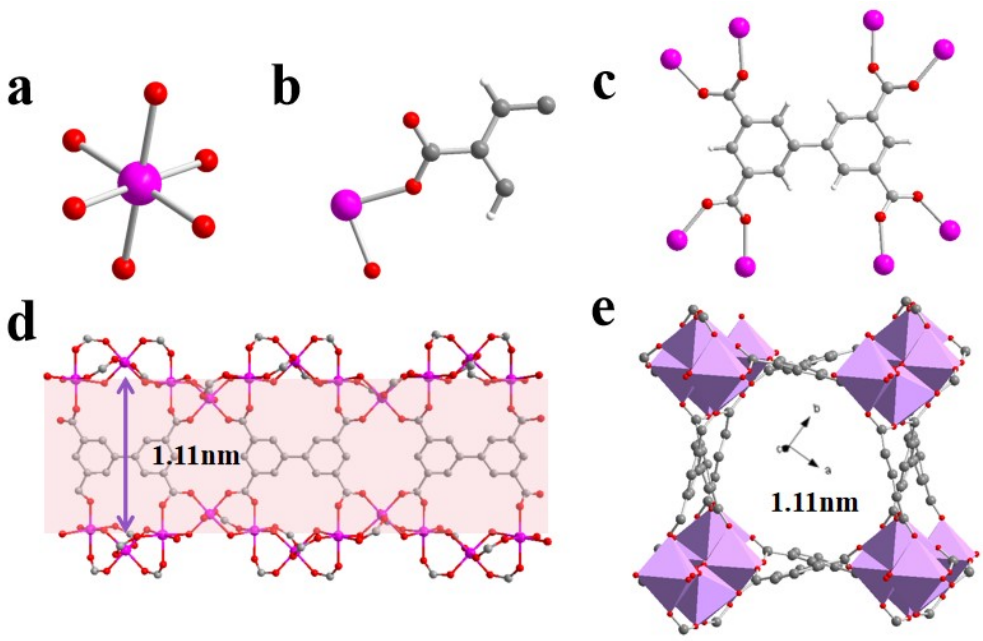

Fig. S1 a) The asymmetry unit, b) 6-coordinated Co(II) center, c) the coordination condition of fully deprotonated $BPTC^{4-}$ ligand, d-e) the tetragonal channels of **CoOF-1**. (H atoms are shown in white, C atoms in gray, O atoms in red, Co ions in pink).

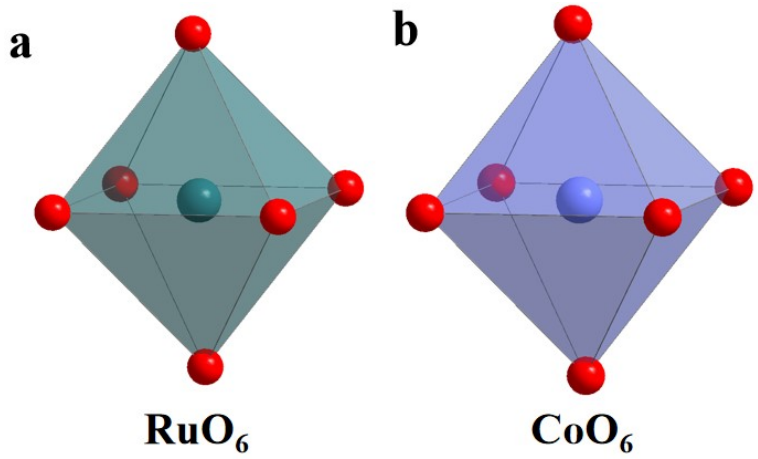

Fig. S2 The similar coordination environments of 6-coordinated (a) Ru and (b) Co.

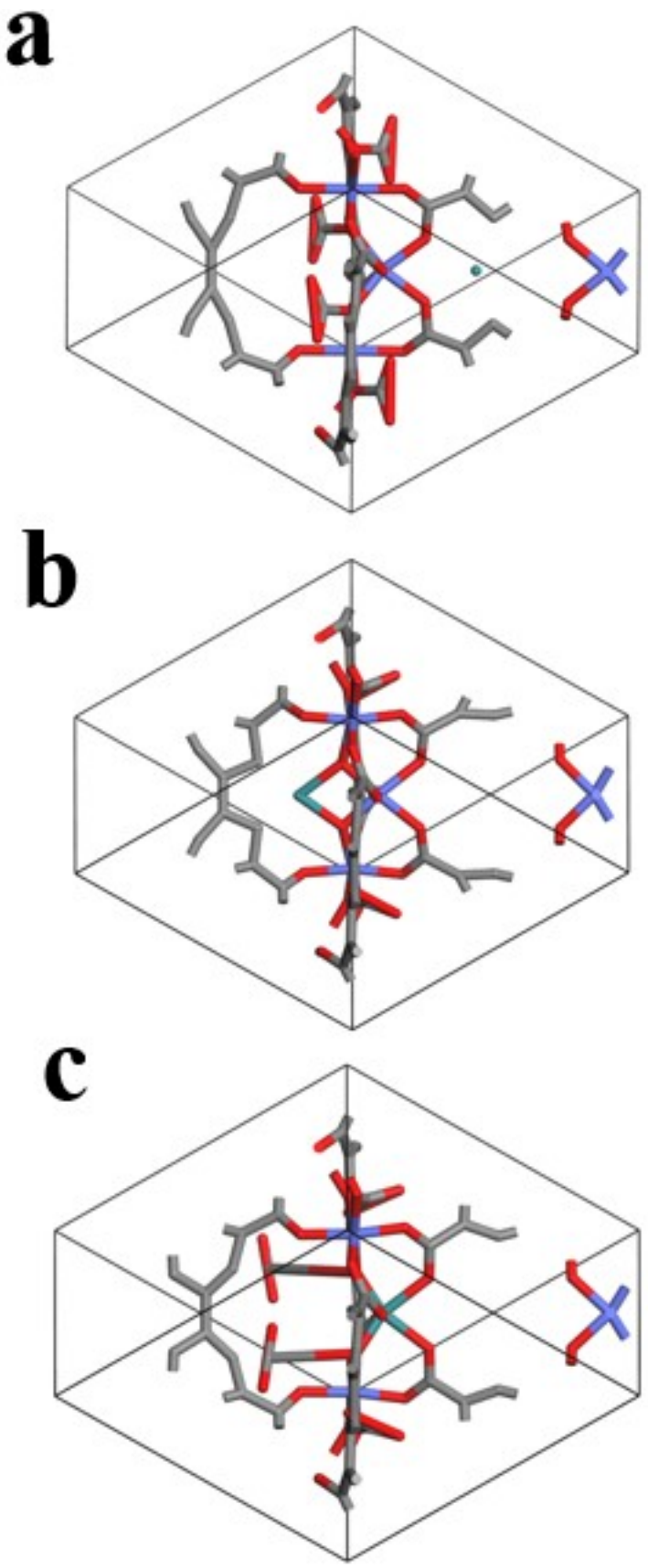

Fig. S3 Three kinds of Ru atoms are anchored in the structure of **CoOF-1**: a) in the pore of **CoOF-1**, b) at the edge of Co-O chain, c) in the lattice of Co-O chain.

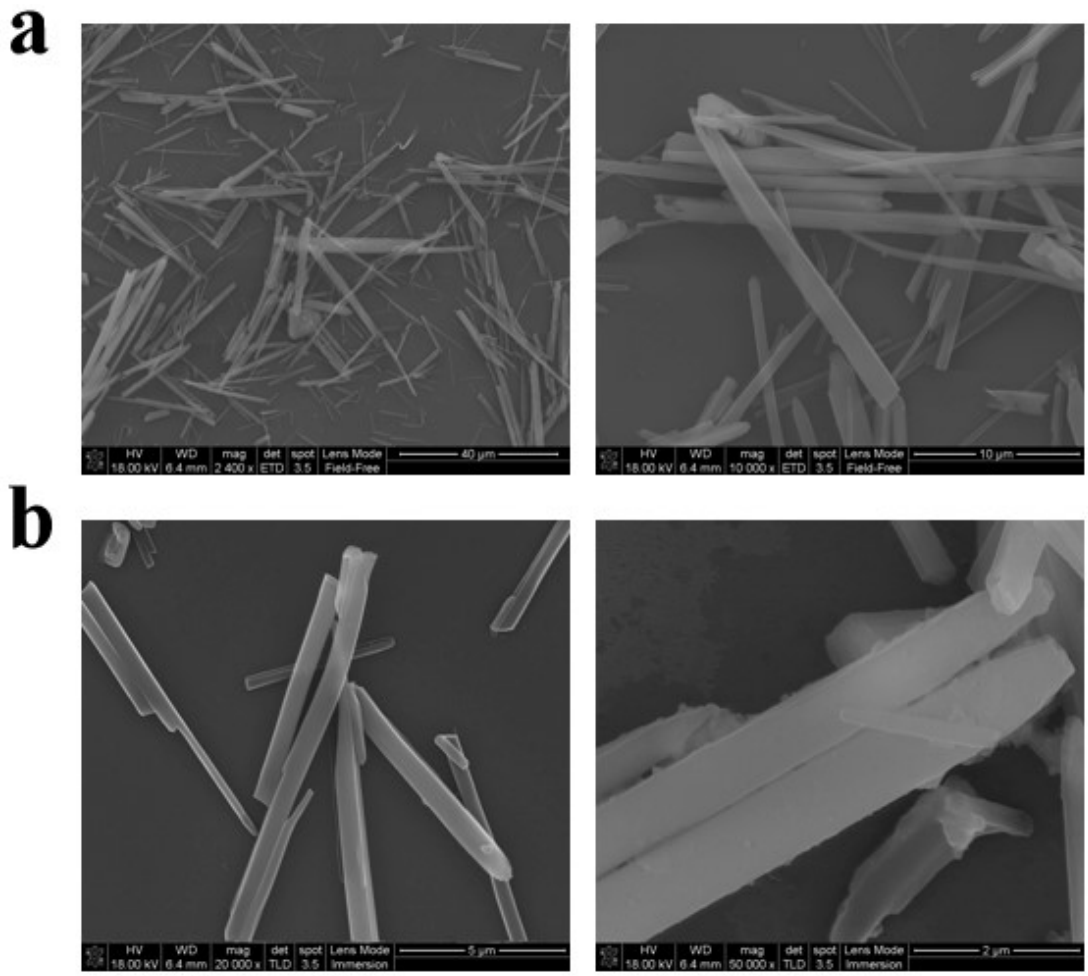

Fig. S4 SEM images of (a) **CoOF-1** and (b) **Ru-CoOF-1**.

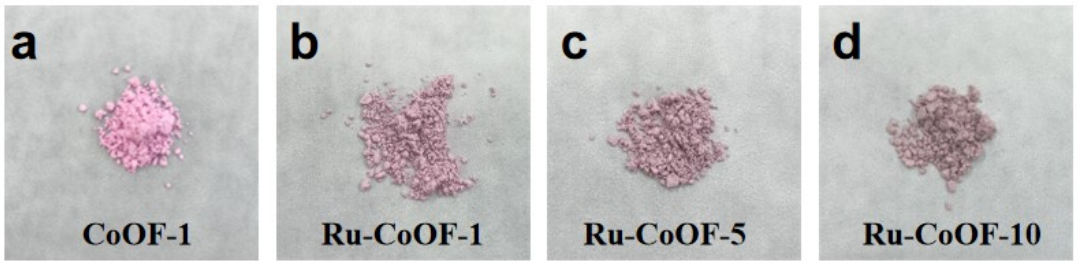

Fig. S5 Digital photographs of (a) **CoOF-1**, (b) **Ru-CoOF-1**, (c) **Ru-CoOF-5** and (d) **Ru-CoOF-10**.

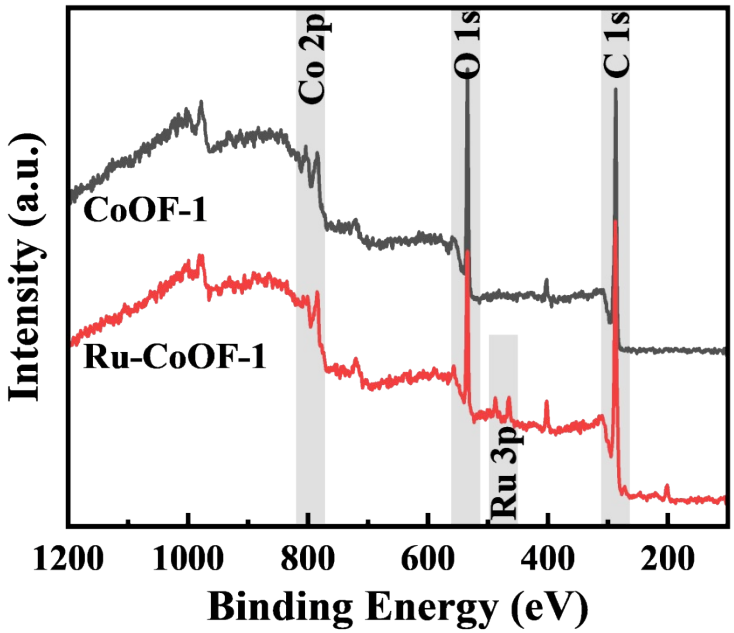

Fig. S6 The full XPS survey spectra of **CoOF-1** (gray) and **Ru-CoOF-1** (red).

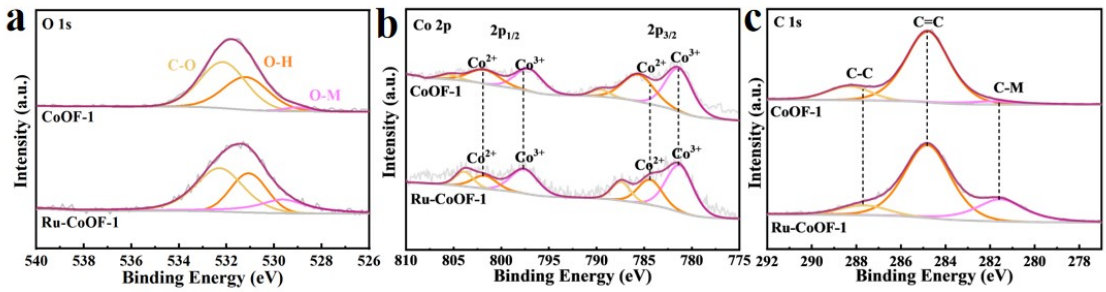

Fig. S7 The high-resolution XPS spectra of a) O 1s, b) Co 2p, and c) C 1s for **CoOF-1** and **Ru-CoOF-1**.

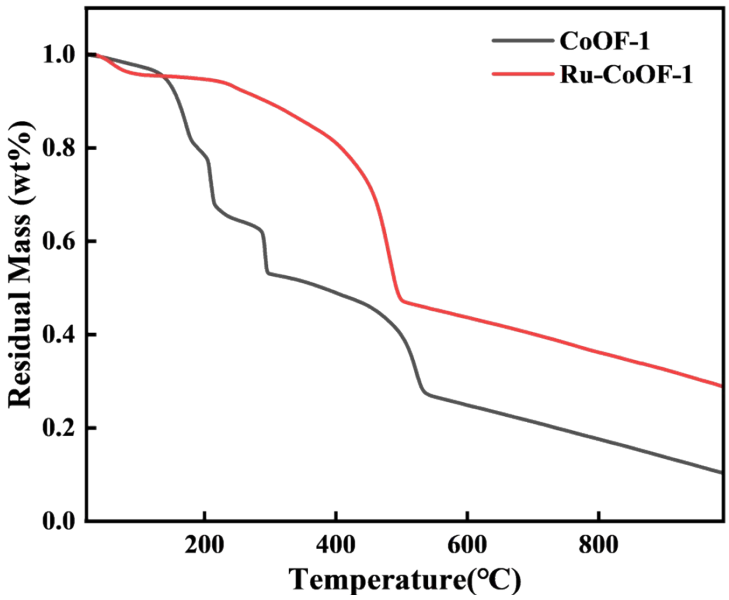

Fig. S8 TGA data of **CoOF-1** and **Ru-CoOF-1**.

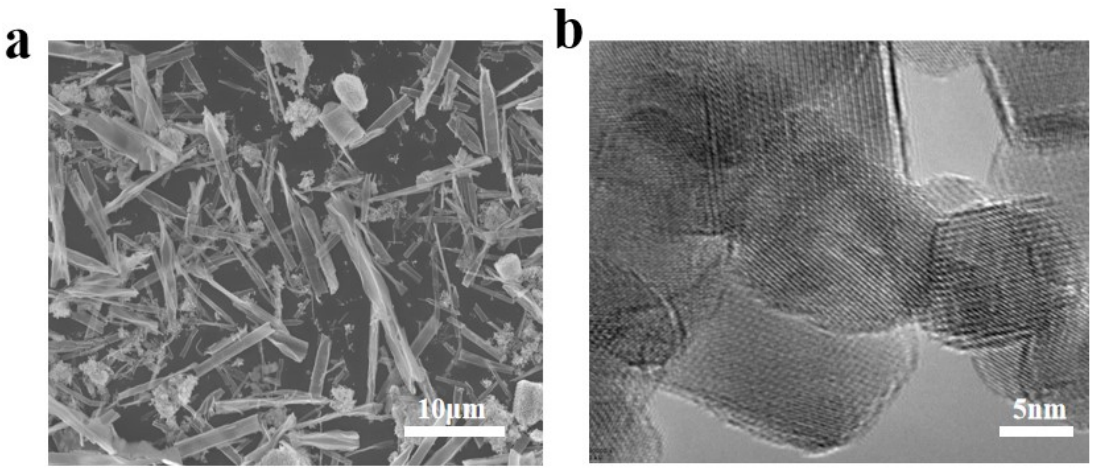

Fig. S9 (a) SEM and (b) HR-TEM images of MOF-derived Co_3O_4.

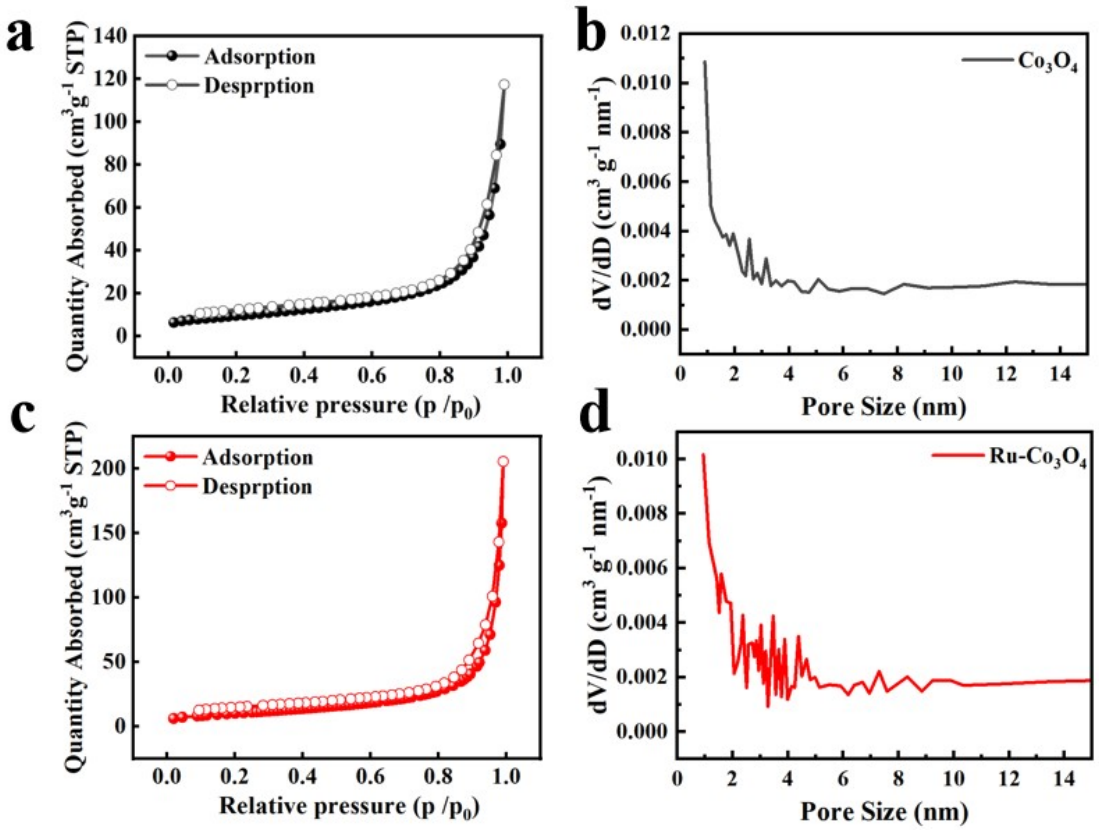

Fig. S10 a) N_2 isotherms, b) Pore size distribution analysis of **Co_3O_4**, c) N_2 isotherms, d) Pore size distribution analysis of **Ru-Co_3O_4**.

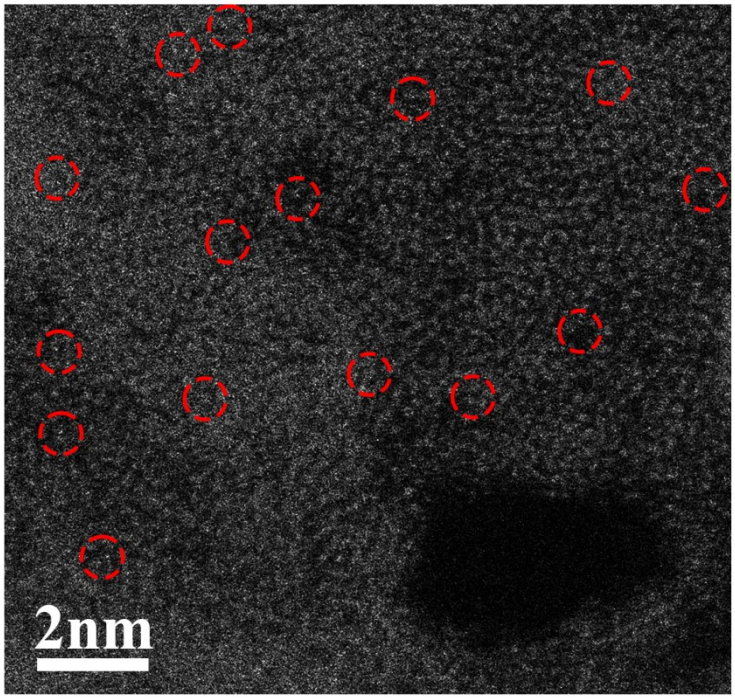

Fig. S11 HAADF-STEM images of MOF-derived Ru-doped Co_3O_4 (**Ru-Co_3O_4-5**).

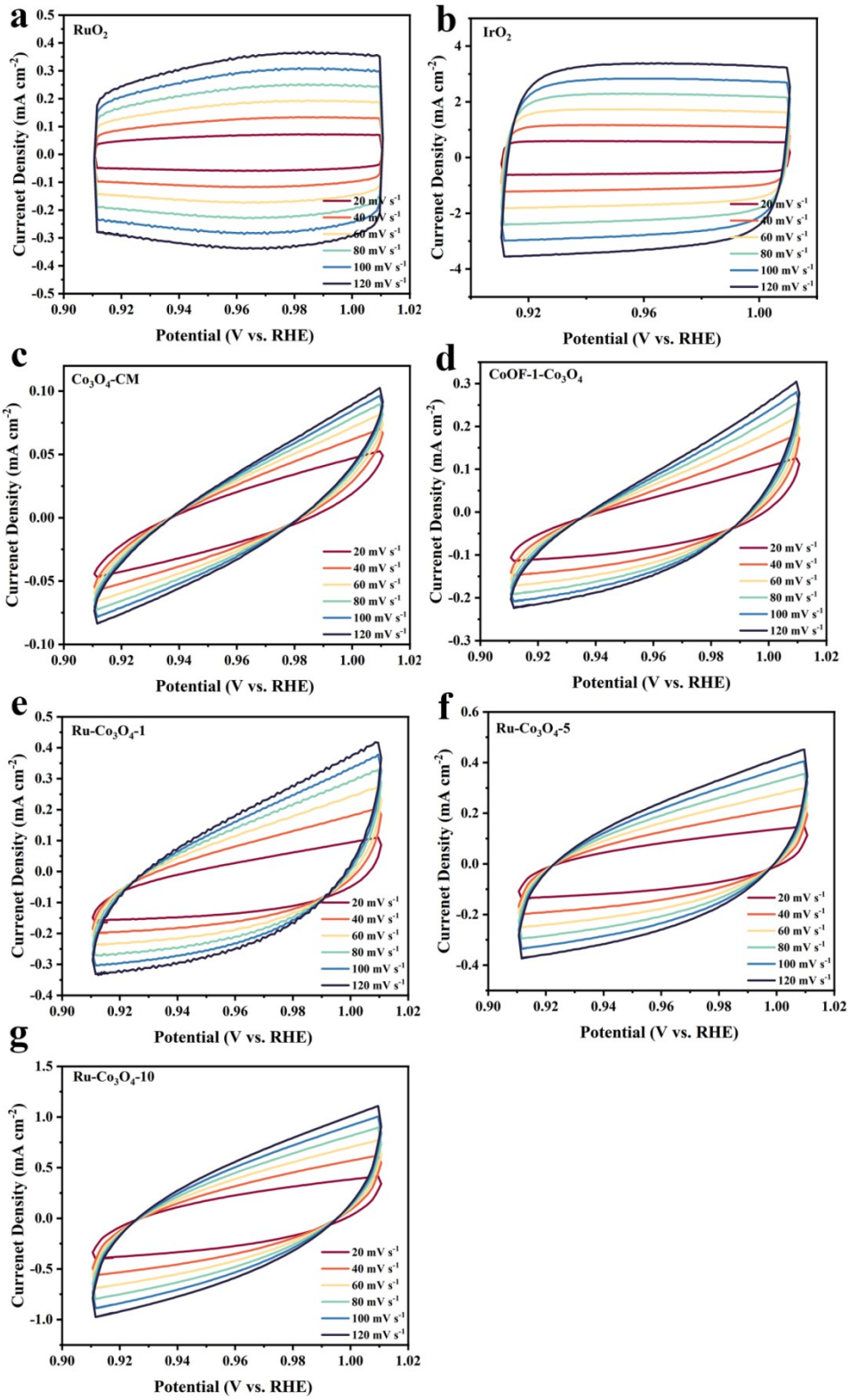

Fig. S12 The double-layer capacitance (C_{dl}) is calculated from the cyclic voltammograms of the a) RuO_2, b) IrO_2, c) Co_3O_4-CM, d) CoOF-1 derived Co_3O_4, e) **Ru-Co_3O_4-1**, f) **Ru-Co_3O_4-5**, g) **Ru-Co_3O_4-10**.

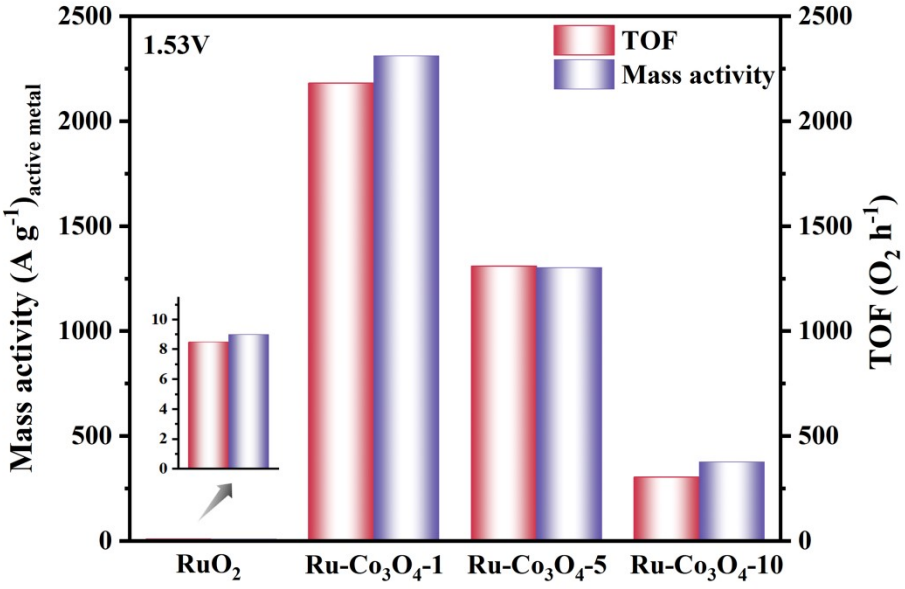

Fig. S13. Mass activity and turnover frequency (TOF) of Ru-Co_3O_4-1, Ru-Co_3O_4-5, Ru-Co_3O_4-10 and RuO_2.

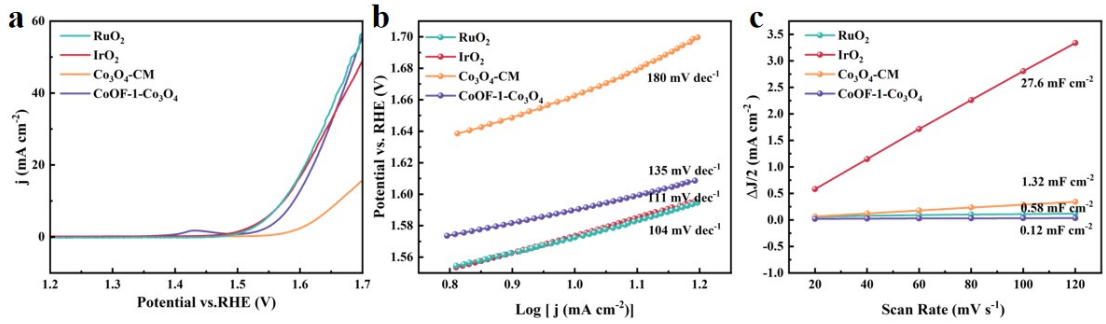

Fig. S14. (a) LSV curves, (b) Tafel slopes, (c) C_{dl} profiles of MOF-derived OER catalysts and commercial catalysts.

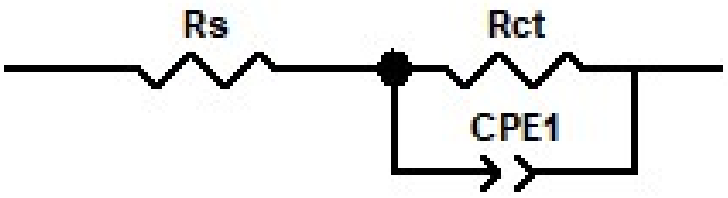

Fig. S15 The equivalent electrical circuit for EIS data (Rs: solution resistance; Rct and CPE1: resistance and CPE impedance of electrical double layer at the interface of activated product layer and GCE substrate).

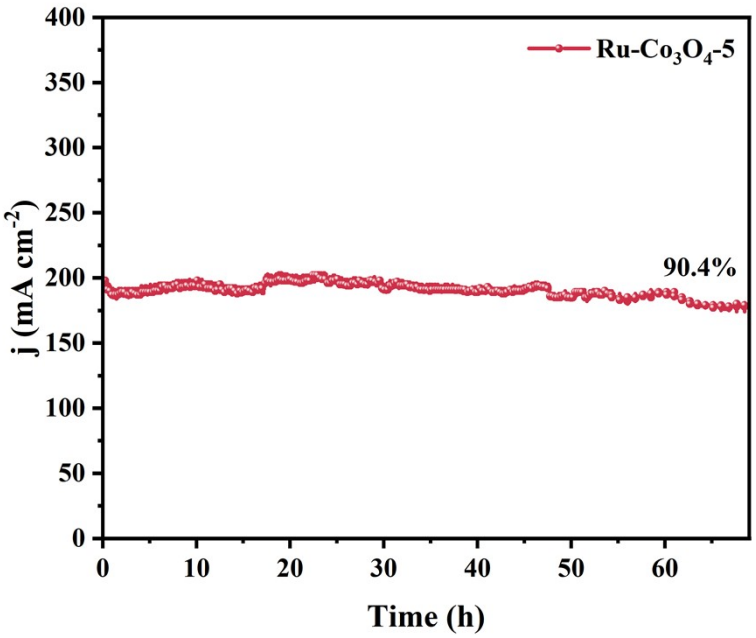

Fig. 16. The current density retention after long-term durability of OER test.

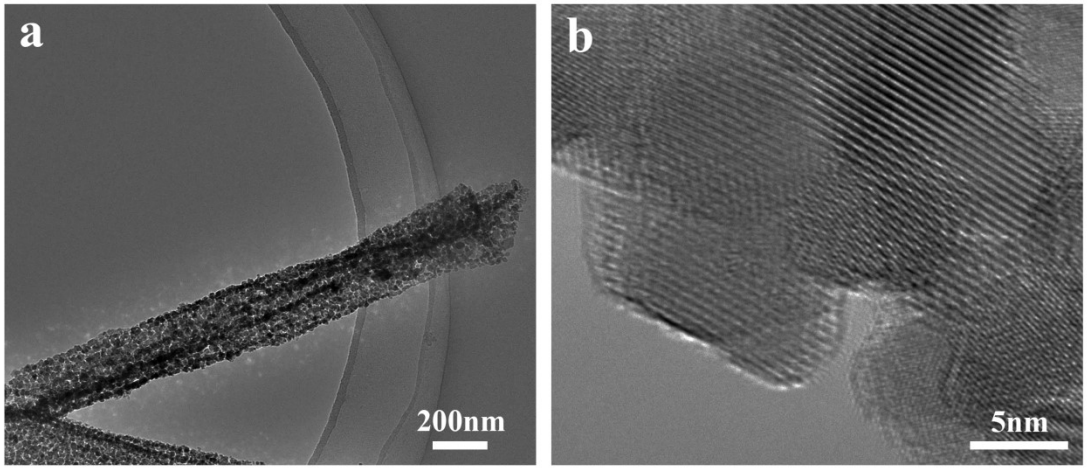

Fig. 17. a) and b) TEM images of Ru-Co_3O_4-5 after long-term test.

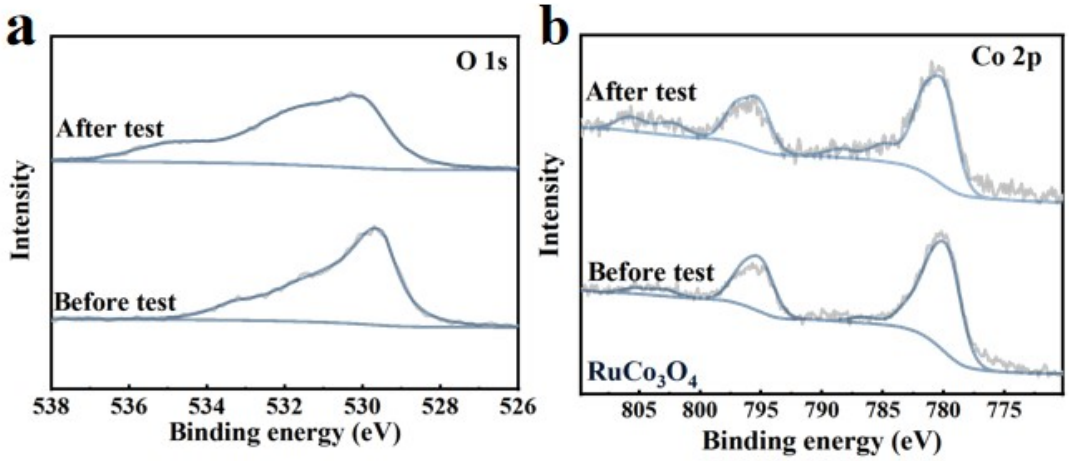

Fig. S18 a) O 1s and b) Co 2p XPS spectra of the **Ru-Co_3O_4-5** before and after the chronopotentiometry test.

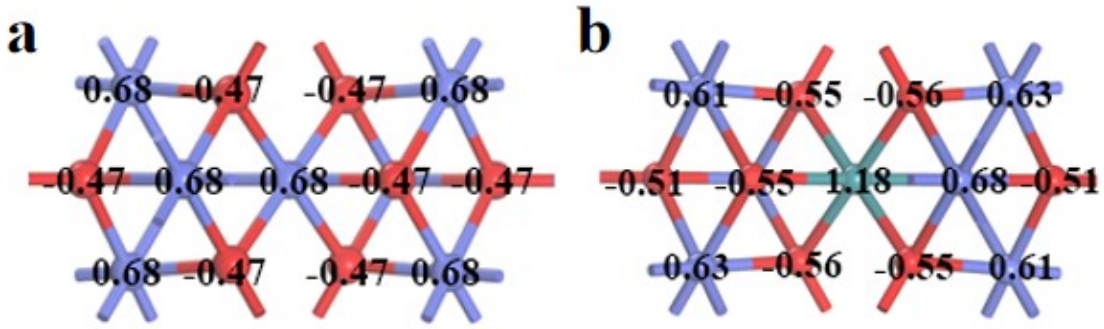

Fig. S19 The electron distribution in the (a) Co_3O_4 model and (b) **Ru-Co_3O_4** model.

Table S1 Summary of Crystal Data for CoOF-1.

Items	**CoOF-1[Ref]**
CCDC	1912147
Formula	$(C_{18}\ H_8\ Co_2\ O_{12})n$
Mass	547.15
crystal system	Tetragonal
Space group	*I4₁22*
a(Å)	15.327 (3)
b(Å)	15.327 (3)
c(Å)	12.270 (3)
α(°)	90.00
β(°)	90.00
γ(°)	90.00
V(Å^3)	2882.6 (13)
T(K)	296
Z	8
F(000)	1128.0
R_{int}	1.158
R_1(I>2σ(I))	0.0310 (1749)
wR_2(all reflections)	0.0866 (1811)

Ref: Li Zhong, Junyang Ding, Xian Wang, Lulu Chai, Ting-Ting Li, Kongzhao Su, Yue Hu, Jinjie Qian, Shaoming Huang CCDC 1912147: Experimental Crystal Structure Determination, 2020, DOI: **10.5517/ccdc.csd.cc225r56**

Table S2 Micropore Volume, Total Pore Volume and Specific Surface Area over All Prepared Catalysts.

Samples	Micropore volume ($cm^3\ g^{-1}$)	Total pore volume ($cm^3\ g^{-1}$)	Specific surface area ($m^2\ g^{-1}$)
CoOF-1	0.0116	0.1120	46.4348
Ru-CoOF-1	0.0189	0.1910	34.4143
Co_3O_4	0.0145	0.1383	33.7280
$RuCo_3O_4$	0.0150	0.3181	37.5978

Table S3 The Deconvolution Data of Co, O, and Ru Atoms in Ru-Co_3O_4 and Co_3O_4.

Species	Ru-Co_3O_4	Co_3O_4
Co^{3+} 2p3/2	779.4	779.7
Co^{2+} 2p3/2	781.2	781.3
Co^{3+} 2p1/2	794.7	794.7
Co^{2+} 2p1/2	796.4	796.4
O_L	529.8	529.9
O_V	531.6	532.0
O_C	533.2	533.2
Ru 3p	463.0	/

Table S4 The Content of Ru in Ru-Co_3O_4 by ICP-OES Measurement.

Catalysts	Relative content of ruthenium (wt.%)
Ru-Co_3O_4-1	0.52
Ru-Co_3O_4-5	3.05
Ru-Co_3O_4-10	8.26

Table S5 The Electrochemical Data of Ru-Co_3O_4 Series.

Samples	Overpotential (mV, η_{10})	Tafel slope (mV dec^{-1})	C_{dl} value (mF cm^{-2})	charge transfer resistance (Ω)
Ru-Co_3O_4-1	319	121	1.58	13.6
Ru-Co_3O_4-5	260	84	3.17	13.5
Ru-Co_3O_4-10	281	96	2.78	11.8
RuO_2	342	104	0.58	17.2
IrO_2	343	111	27.6	
CoOF-1-Co_3O_4	360	135	0.12	15.3
Co_3O_4-CM	433	180	1.32	

Table S6 OER Performance Comparison between Ru-Co_3O_4 and Other Electrode Materials.

Samples	Electrolyte	η10 (mV)	Tafel slope (mV dec^{-1})	Reference
Ru-Co_3O_4-5	1.0 M KOH	260	84	
Ru-Co_3O_4-1	1.0 M KOH	318	121	**This Work**
Ru-Co_3O_4-10	1.0 M KOH	280	96	
Ir0.33@Co_3O_4	1 M KOH	296	68	ACS Catal., **2022**, 12, 13482−13491.
Co_3O_4 NC	1 M KOH	380	101	Angew. Chem., Int. Ed., **2020**, 59, 7245−7250.
Ir/Co	1 M KOH	273	99	J. Mater. Chem. A **2019**, 7, 8376-8383.
IrCo-NC	0.1 M KOH	330	79	ACS Catal. **2021**, 11, 8837-8846
Fe adsorbed CoOx	1 M KOH	309	27.6	*ACS Catal.* **2018**, *8*, 807-814
Co/C_3N_4@CNT	1 M KOH	380	68.4	J. Am. Chem. Soc. **2017**, 139, 3336-

				3339
CoIr-0.2	1 M KOH	235	70.2	*Adv. Mater.* **2018**, *30*, 1707522.
Zn0.2Co0.8OOH	1 M KOH	235	34.7	*Nat. Energy* **2019**, *4*, 329-338
NiCo LDHs	1 M KOH	334	41	*Nat. Commun.* **2014**, *5*, 4477.